Electronic Supplementary Material (ESI) for Inorganic Chemistry Frontiers.
This journal is © the Partner Organisations 2021

Supporting Information

Carbon-Doping Induced Energy Band Modification and Vacancy in SnS_2 Nanosheets for Room-temperature ppb-Level NO_2 Detection

*Ruozhen Wu[a], Juanyuan Hao[*a,b], Tingting Wang[a], Shengliang Zheng[a] and You Wang [*a,b]*

[a]School of Materials Science and Engineering, Harbin Institute of Technology, Harbin 150001, P. R. China.

[b]Key Laboratory of Micro-Systems and Micro-Structures Manufacturing, Ministry of Education, Harbin 150001, P. R. China

*E-mail: jyhao@hit.edu.cn and y-wang@hit.edu.cn

Fig. S1 Homemade chemical gas sensing analysis system. The gas test box is placed in a cyclic damp heat test instrument (left) with the controllable temperature and relative humidity.

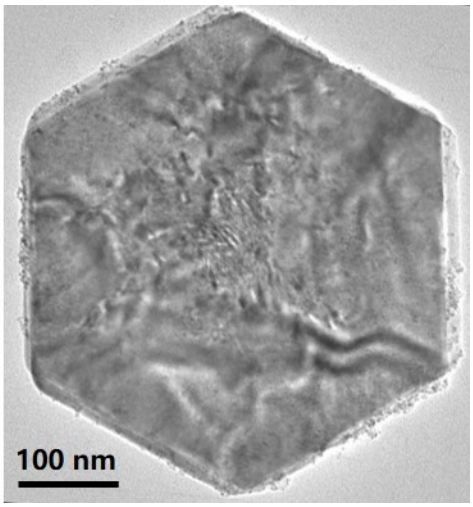

Fig. S2 TEM image of pristine SnS_2. The morphology of pristine SnS_2 showed hexagonal plate-like structure with uniform lateral size of ~400 nm.

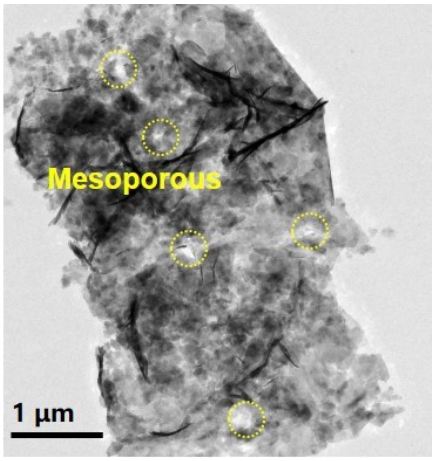

Fig. S3 TEM image of the C-SnS_2-32 sample. It indicates the obvious mesoporous nanostructures in the C-SnS_2-32 nanosheets.

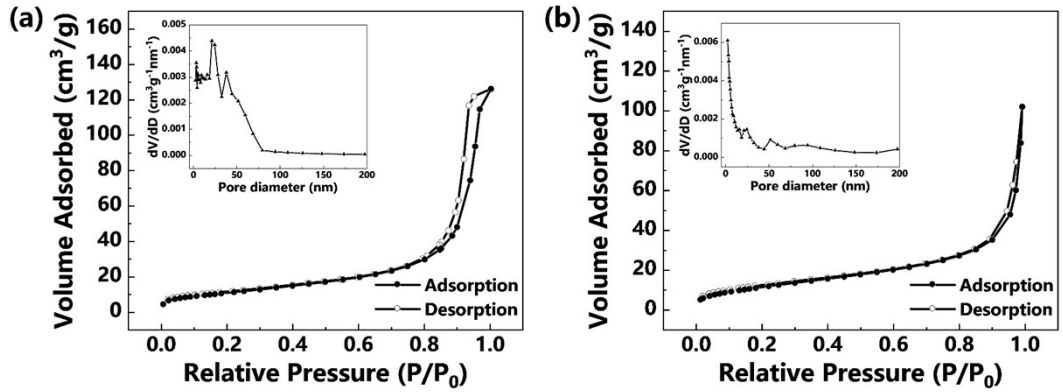

Fig. S4 N_2 sorption isotherms at 77 K of (a) C-SnS_2-32 and (b) pristine SnS_2. The BET surface area of C-SnS_2-32 nanosheets was measured to be 26.6 m^2g^{-1}, which was 2.5 times larger than that of pristine SnS_2 (10.7 m^2g^{-1}), which indicates that the adsorption capacity of NO_2 is improved on the C-doped SnS_2 surface.

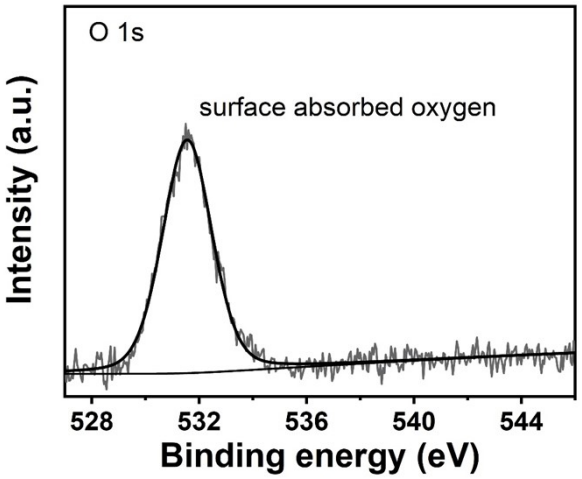

Fig. S5 High-resolution O 1s XPS spectra for the C-SnS_2-32. The peak centred at 531.9 eV is assigned to the surface adsorbed oxygen.[1,2]

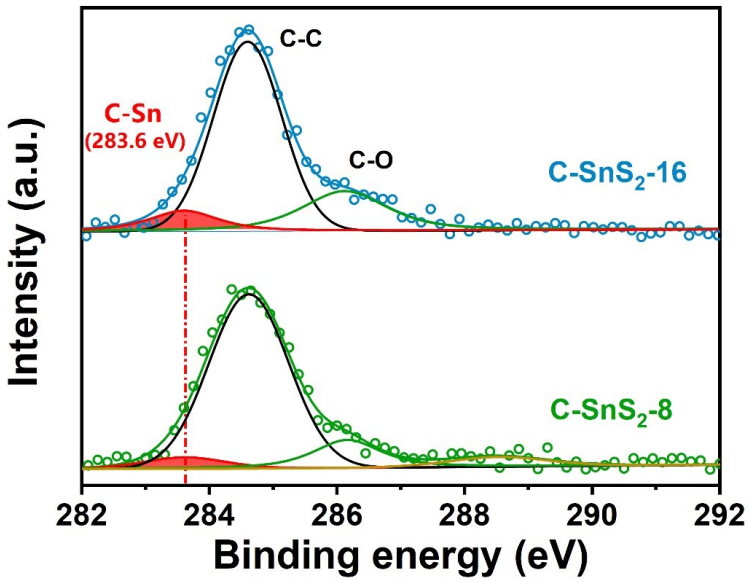

Fig. S6 High-resolution C 1s XPS spectra for C-SnS_2-8 and C-SnS_2-16. The clear signal of C-Sn bond is also found in both of C-SnS_2-8 and C-SnS_2-16, confirming the presence

of C doping in SnS_2.

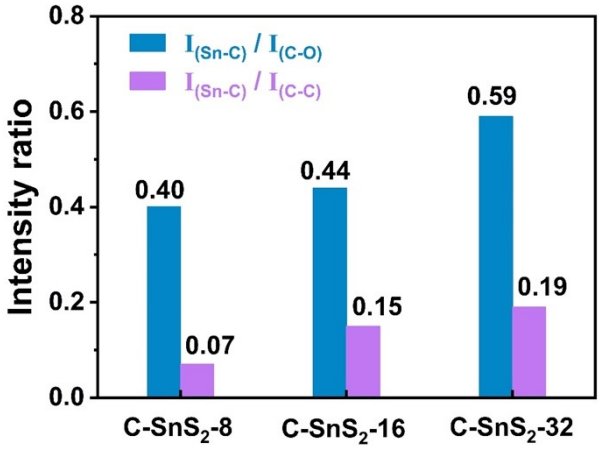

Fig. S7 The peak intensity ratios of Sn-C with C-O and C-C for C-doped SnS_2. The peak intensity ratios of the Sn-C/C-C and the Sn-C/C-O increase from C-SnS_2-8 to C-SnS_2-32, indicating the content of Sn-C bond increases with C dopants concentration while the C-C and C-O peaks does not change.

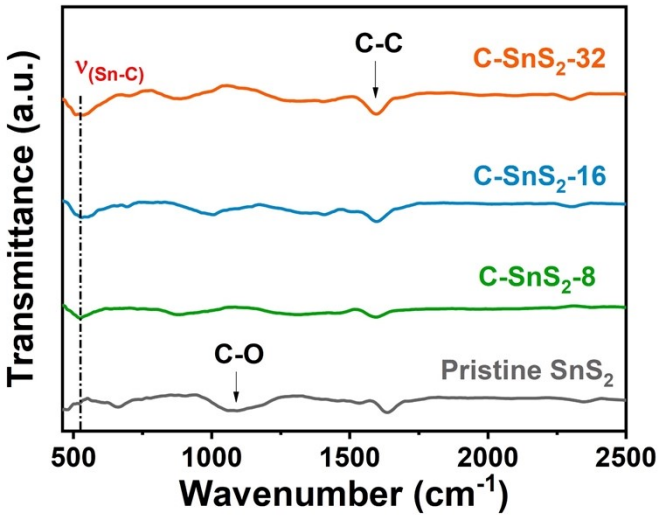

Fig. S8 FT-IR spectra of pristine SnS_2, C-SnS_2-8, C-SnS_2-16, and C-SnS_2-32. The peak at ~520 cm^{-1} for C-doped SnS_2 is assigned to the Sn-C stretching, which is absent in pristine SnS_2, supporting that C is doping into SnS_2 crystals.

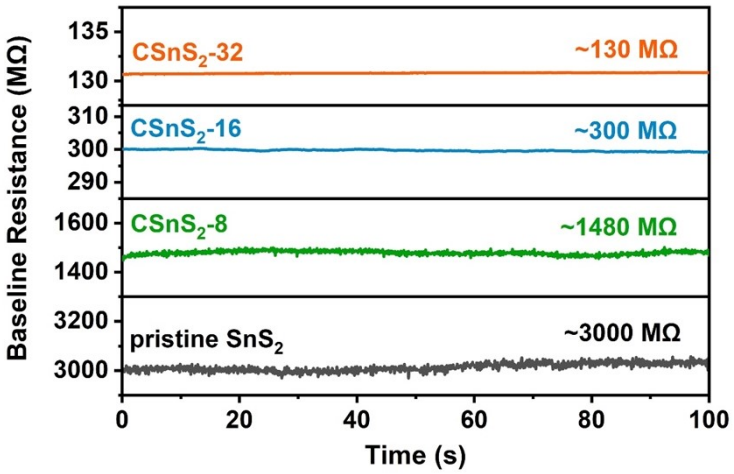

Fig. S9 Baseline resistance of pristine SnS_2, C-SnS_2-8, C-SnS_2-16, and C-SnS_2-32. The baseline resistance sharply declined after C doping, from ~3000 MΩ of pristine SnS_2 to ~130 MΩ of C-SnS_2-32, indicating that the C doping dramatically enhanced the electron concentration and the conductivity of SnS_2.

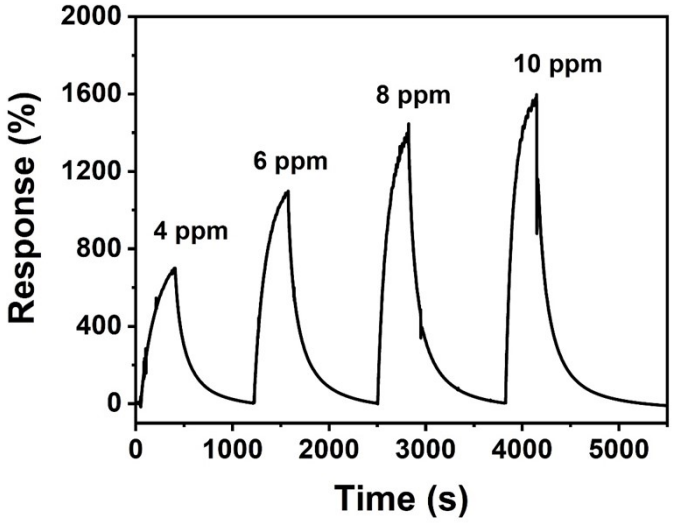

Fig. S10 Dynamic response-recovery curve of C-SnS_2-32 to diverse NO_2 concentrations from 4 ppm to 10 ppm . The result indicates that the response value of C-SnS_2-32 sensor increases with increasing NO_2 concentration and the signal completely returns to initial state after NO_2 release.

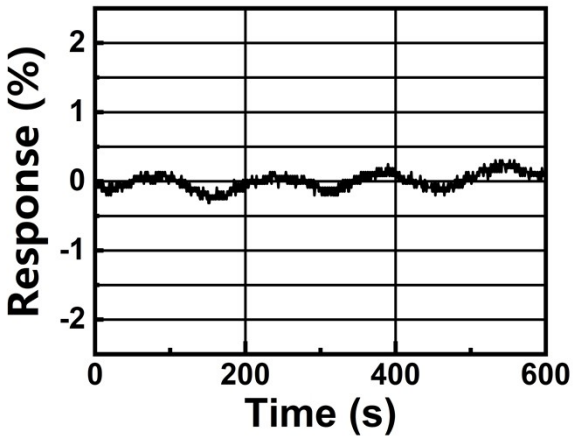

Fig. S11 A temporal trace of experimentally recorded noise of response for .the sample C-SnS_2-32. The result indicates that the root-mean-square value of response noise is approximate ~0.12%.

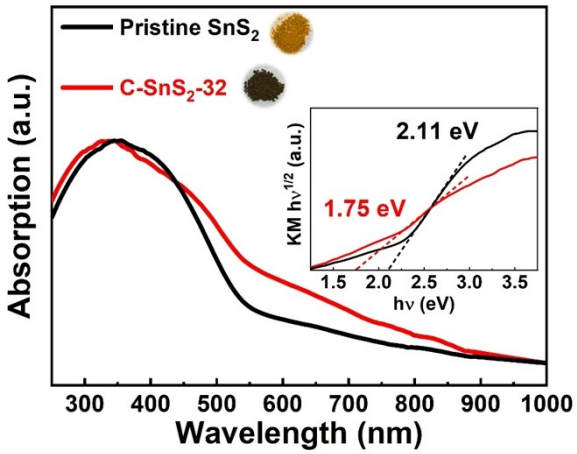

Fig. S12 UV-Vis diffuse reflectance spectroscopy of the C-SnS_2-32 and pristine SnS_2.The inset of is Tauc plot with indirect bandgap fitting. The characterization of UV-Vis diffuse reflectance spectroscopy indicates the conspicuously narrowed bandgap structure from 2.11 to 1.75 eV after C doping.

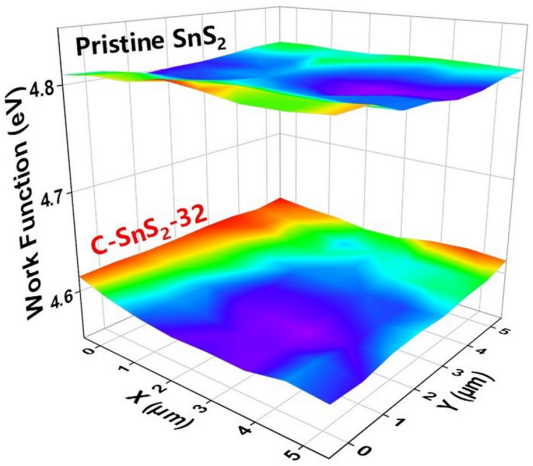

Fig. S13 KPFM measured work function area scans of the C-SnS_2-32 and pristine SnS_2. The measurement of KPFM indicates the elevation of Fermi energy level from 4.81 to 4.61 eV after C doping.

References

[1] H. Chen, Y. Zhao, L. Shi, G.-D. Li, L. Sun and X. Zou, Revealing the relationship between energy level and gas sensing performance in heteroatom-doped semiconducting nanostructures, *ACS Appl. Mater. Interfaces*, 2018, **10**, 29795-29804.

[2] Q. Yang, Y. Wang, J. Liu, J. Liu, Y. Gao, P. Sun, Z. Jie, T. Zhang, Y. Wang and G. Lu, Enhanced sensing response towards NO_2 based on ordered mesoporous Zr-doped In_2O_3 with low operating temperature, *Sens, Actuators, B*, 2017, **241**, 806-813.